**USING MARS ORBITAL CAMERA DUST DEVIL OBSERVATIONS TO DEVELOP SCHEMES FOR REPRESENTING DUST DEVILS IN MARS GENERAL CIRCULATION MODELS.** N.G. Heavens[1], M.I. Richardson[1], and C.E. Newman[1] [1]Division of Geological and Planetary Sciences, California Institute of Technology, MC 150-21, Pasadena, CA, 91125 (heavens@gps.caltech.edu, mir@gps.caltech.edu, claire@gps.caltech.edu)

**Introduction:** If the chief concern of the terrestrial weather forecaster is the hydrometeor, i.e., rain, snow, sleet, hail, and fog, the chief concern of future Martian weather forecasters likely will be the coniometeor, i.e., dust. Dust lifted by the dry convective vortices commonly known as "dust devils" and by the larger scale systems known as "dust storms" may present a variety of hazards to both robotic and human exploration of Mars ranging from low visibility to the exotic and corrosive possibility of transient peroxide deposits synthesized in the strong electric fields associated with dust lifting activity [1].

While the effects of dust devils and dust storms on human exploration are mostly speculative, the effects of atmospheric dust on the radiative properties and dynamics of the Martian atmosphere are quite well-observed. Atmospheric dust scatters and absorbs both visible and infrared radiation, significantly affecting local temperatures in areas of high concentration [2]. Although feedbacks between dust concentration and large-scale dynamics probably are important only in the vicinity of dust storms, dust devil activity probably sets the background dust concentration and thus atmospheric temperatures. In addition, being able to quantify present dust lifting and deposition and hindcast it in the past would be of interest to sedimentologists and geomorphologists.

Therefore, for both Martian weather forecasting and a variety of scientific problems related to the Martian atmosphere and its modification of the surface, it is critical that we have an accurate way to represent dust lifting activity in a Mars General Circulation Model (GCM). In this abstract, we seek a scheme to represent the dust devil number density, i.e., the number of dust devils per unit area, in a GCM. We first briefly review a common approach to the problem of dust devil representation in general and present an alternative scheme. We then use dust devil density data from Cantor et al. [3] and output from the Mars implementation of the Planetary Weather Research and Forecasting model (MarsWRF) [4] to investigate the relationship between dust devil number density and particular formulations of boundary layer instability or available thermodynamic energy. Finally, we discuss an important limitation of this analysis, our limited knowledge of the atmospheric roughness properties of Mars, and its implications for present and future work.

**Representing Dust Lifting by Dust Devils:** During the last few generations of Mars GCMs, there has been a need to parameterize the dust flux due to dust devil activity for the purpose of "active dust" simulations, in which the model simulates the lifting and transport of dust throughout the atmosphere and its radiative effects [5]. A common scheme uses Renno et al.'s hypothesis [6] that the limitation on dust devil activity is the amount of thermodynamic energy available if the convective boundary layer is treated as a Carnot heat engine. The scheme then assumes this proportionality is linear and further assumes that dust devil activity and the flux of lifted dust are likewise linearly related, making dust flux linear in available thermodynamic energy in the boundary layer [2]. However, the confirmation of Renno's hypothesis on Mars by observations remains debatable [1, 7] and the assumptions of linearity remain unjustified.

**An Alternative Scheme: The Simple, Steady-State Nucleation Model:** Fisher *et al.* [7], based on Mars Global Surveyor (MGS) Mars Orbital Camera (MOC) imagery and temperature profiles retrieved from MGS Thermal Emission Spectrometer (TES) data, hypothesized that there might be some critical threshold of available thermodynamic surface heat flux above which dust devils form. Investigators of terrestrial dust devils also have considered critical instability conditions for dust devil formation [8]. Let us suppose that the mean Martian boundary layer on a typical GCM grid scale O(100-500 km.) is below some critical instability condition, $\chi_c$ measured in terms of an atmospheric metric $\chi$. However, this condition is exceeded locally on length scales no larger than the atmospheric boundary layer thickness O(1-10 km.). Thus, a typical grid box is divisible into 1000-25000 sub-cells, which differ somewhat in $\chi$. For mathematical simplicity, we assume that $\chi$ follows a Boltzmann distribution. We intend to test this hypothesis in future work, but the major underlying assumptions of this simplification are that vertical eddy diffusion of heat dominates horizontal advection and that the nonlinearity of $\chi$ is limited. Then, by analogy with chemical kinetics, formation of a dust devil can be modeled like a first order chemical reaction in the "reactant" $\chi$, i.e., the nucleation of dust devils is a negative exponential function of the quotient of $\chi_c$ and the mean $\chi$ of the grid box, $\chi^*$. We next approximate the dissipation rate of dust devils to be $= N_{DD}/T_{DD}$, where $N_{DD}$ is their number density and $T_{DD}$ is the dust devil lifetime, which we approximate as the vertical mixing time of

the dust devil circulation as suggested by the results of large eddy simulations [9] rather than the horizontal mixing time as proposed by Greeley and Iversen [10]. We next assume that over the grid cell, the nucleation and dissipation of dust devils is in steady state. Then the dust devil density, $N_{DD}$ can be parameterized as:

$$N_{DD} = kT_{DD} \exp\left(-\frac{\chi_c}{\chi^*}\right) \quad (1)$$

k is a proportionality constant, which represents the nucleation rate in exceptionally favorable conditions. If we have estimates of $T_{DD}$ and $\chi^*$, we can develop a parameterization scheme for $N_{DD}$ by re-arranging (1) and fitting $\chi^*$ to an observational record of $N_{DD}$ to solve for the unknown parameters k and $\chi_c$:

$$\ln\left(\frac{N_{DD}}{T_{DD}}\right) = \ln(k) - \chi_c\left(\frac{1}{\chi^*}\right) + \varepsilon \quad (2)$$

Note that this model ignores uncertainty in $N_{DD}/T_{DD}$.

**Developing Experimental $N_{DD}$ Parameterization Schemes for MarsWRF:** In order to perform the regression outlined in (2), we ran GCM simulations using MarsWRF for several model years using an idealized passive dust forcing based on retrievals from MGS TES (MGS Mapping Year 1) described in [11]. In other words, the parameterization schemes have no effect on the model forcing. All model output used in this study is from the fourth model year of the simulation, but the correlation between quantities calculated from output in the fourth and fifth model years is statistically significant to an exceptionally high confidence. Any interannual variability in the model is primarily due to weather noise, especially from high-latitude northern hemisphere wave activity. The vertical grid used is the Oxford/LMD grid, which has suitable density of model layers near the surface.(~5 m., ~22 m., ~ 50 m., ~105 m. etc.). It is relatively easy to program MarsWRF to calculate quantities not normally calculated in the model. A good example of this kind of quantity is $T_{DD}$, which we define as equal to $h^{1/2}D^{1/2}/(w_{DD}+|w_1|)$, where h is the convective boundary layer height, $w_{DD}$ is the vertical convective velocity of the dust devil is calculated according to Renno et al.'s method [6], and $w_1$ is the vertical velocity within the first model layer. D we call the characteristic superadiabatic layer and define it as:

$$D = \frac{k_{z1}\rho c_p(\theta_s - \theta_{TBL})}{F_s} \quad (3)$$

where $k_{z1}$ is the vertical eddy diffusivity of the first model layer, $\rho$ is the air density, $c_p$ is the specific heat capacity of Martian air, $F_s$ is the surface heat flux, and $\theta_s$-$\theta_{TBL}$ is the superadiabatic temperature excess of the boundary layer, the difference between the potential temperature of the surface (if it were a gas), $\theta_s$, and the potential temperature at the top of the boundary layer, $\theta_{TBL}$. The reference pressure is 610 Pa.

We test three possibilities for $\chi_c$. First, we test Fisher et al.'s hypothesis [7] that there is some critical available thermodynamic surface heat flux ($\Lambda_c$) below which dust devils do not form. Following Renno et al. [6], $\Lambda$ is defined as $\eta F_s$, where $\eta$ is the thermodynamic efficiency of the boundary layer. Second, we test the hypothesis of Hess and Spillane [8] that there is some critical (–h/L) or $De_c$ (critical Deardorff number) below which dust devils do not form. L is the Obukhov length, usually interpreted as the thickness of the near-surface layer of mechanical turbulence. Third, we test the hypothesis of Cortese and Balachandar [14] that there is some critical Rayleigh number, $Ra_c$, above which dust devils arise as coherent structures within hard turbulence. In this case, Ra is the Rayleigh number of the characteristic superadiabatic layer: $g(\theta_s-\theta_{TBL})D^3/(\theta_1\nu\kappa)$, where $\theta_1$ is the potential temperature of the first model layer, and $\nu$ and $\kappa$ are the molecular diffusivities of momentum and heat respectively. The two latter quantities are treated as linear functions of temperature derived from published values for carbon dioxide at low pressure [13].

$N_{DD}$ data, which we will call $N_{DDWA}$, come from dust devil counts reported by Cantor et al. [3] in MOC Wide Angle imagery. We chose to use this data because of its abundance. However, there are some discrepancies between the MOC image numbers reported in [3] and the latitude and longitude data reported there. In those cases, we did not use the data. We then used the image information from the MOC image databases (both from the Planetary Data System node and Malin Space Systems) to calculate the areas of each image, dividing the dust devil counts by the image areas to obtain $N_{DDWA}$ for three regions with high data density, Amazonis Planitia (~36° N, 160° W, n=247, see Figure 1); Syria-Claritas Fossae (~14° S, 108 W, n=98); and Meridiani Planum (~5° S, 10 ° W, n=30). We use all available data even though in many cases, the data from a site is from different Mars years. This approach probably will not be problematic for Amazonis Planitia, since it is less likely than the other sites to be affected by dust storms during its active dust devil season, so we do not expect significant interannual variability in activity to the first order. However, we expect significant error in $N_{DD}$ (differences between the true dust forcing and the idealized model dust forcing) at the other sites due to dust storm activity, especially since the MOC imagery often was collected in these areas in order to monitor dust storm

activity. We then interpolate the MarsWRF output of $T_{DD}$ and $\chi^*$ to the approximate location, $L_s$, and local solar time (LST) of the $N_{DDWA}$ data.

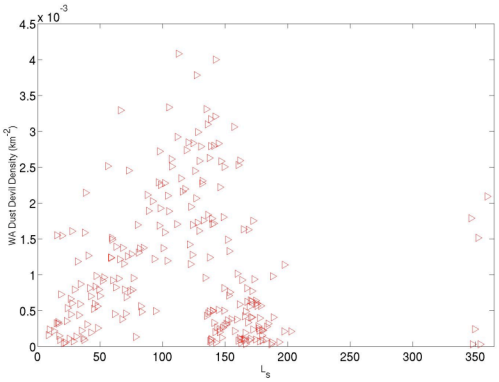


**Figure 1:** $N_{DDWA}$ as a function of $L_S$ at Amazonis Planitia.

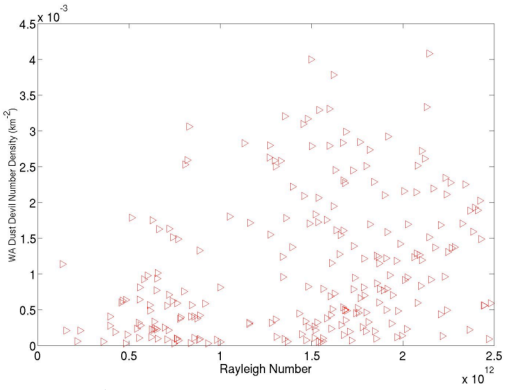


**Figure 2:** $Ra^*$ vs. $N_{DDWA}$ at Amazonis Planitia.

**Correcting the Observations for Size:** We assumed initially that the size spectrum of dust devils was invariant, i.e., the proportion of dust devils resolved in the MOC WA imagery relative to the total number of dust devils was independent of the atmospheric state. However, scatter plots of $\chi^*$ vs, $N_{DDWA}$ tended to peak at intermediate $\chi^*$ (e.g. Figure 2), either suggesting a major defect in our model or some problem with the data. Kurgansky [14] has proposed and given some demonstrations that the probability distribution function of dust devil diameter, $p(D_{DD})$, follows:

$$p(D_{DD}) = \frac{\exp(-D_{DD} / < D_{DD} >)}{< D_{DD} >} \qquad (1)$$

where $<D_{DD}>$, following the data of [8], is $|2L|$. Thus, if we assume a resolved dust devil in MOC WA imagery is 500 m., we can convert $N_{DDWA}$, the WA dust devil density to $N_{DDT}$, the total dust devil density, by multiplying $N_{DDWA}$ by a factor of exp(500/2|L|). Note the improvement in the scatter plot in Figure 2, when this correction is made (Figure 3).

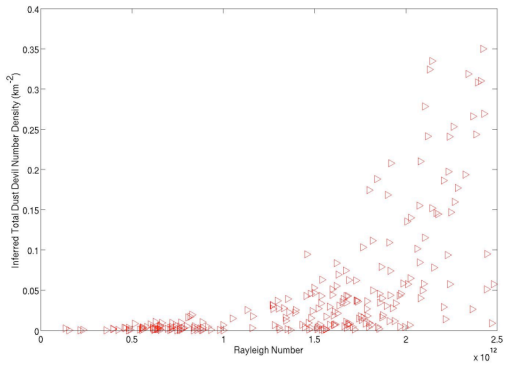


**Figure 3:** $Ra^*$ vs. $N_{DDT}$ at Amazonis Planitia

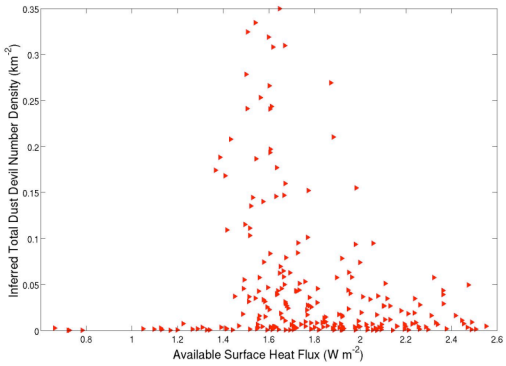


**Figure 4:** $\Lambda^*$ vs. $N_{DDT}$ at Amazonis Planitia

**Which Is the Better $\chi_c$?:** Just examining the scatter plots of $\chi^*$ vs. $N_{DD}$, we saw definite positive exponential relations between $De^*$ and $N_{DDT}$ and $Ra^*$ and $N_{DDT}$. However, the plot of $\Lambda^*$ vs. $N_{DDT}$ again showed a maximum of $N_{DD}$ at intermediate values of $\Lambda^*$ (Figure 4). Note that if $\Lambda$ was the principal limitation on dust devil activity, we would expect some kind of monotonic increase of $N_{DDT}$ with $\Lambda$, which is not observed.

Although $N_{DD}$ appears to be a positive exponential function of $De^*$ as we expect, an ordinary least-squares fit using (2) produces non-random but apparently biased parameters. In other words, the agreement between parameterization scheme using $De^*$ based on the fit and the data is quite imperfect. This problem is not unexpected. Hess and Spillane [8] noted that $De_c$ was not invariant but depended on mechanical forcing conditions. For instance, $De_c$ appeared to be significantly lower in association with density currents and fronts. There is some evidence from observations of dry convection on Earth that $De_c$ and perhaps $Ra_c$ is low under conditions in which the near-surface superadiabatic gradient is driven by strong cold air advection (CAA) [15, 16]. Because CAA might be difficult to resolve on the scale of the standard MarsWRF grid (36 points in latitude and 64 in longitude), we use helicity as a proxy for it. Some physical justification

for the importance of helicity in dust devil development comes from the work of Maxworthy [17], who suggests that a shear state corresponding to negative helicity favors the intensification of cyclonic vortices and vice versa. If we then re-arrange (2) and assume that k is invariant (and thus all points in an Arrhenius plot of 1/De* vs. $\ln(N_{DDT}/T_{DD})$ point to the intercept ln(k), we can estimate k. Then we can solve for $De_c$ and plot it against near-surface helicity (Figure 5).

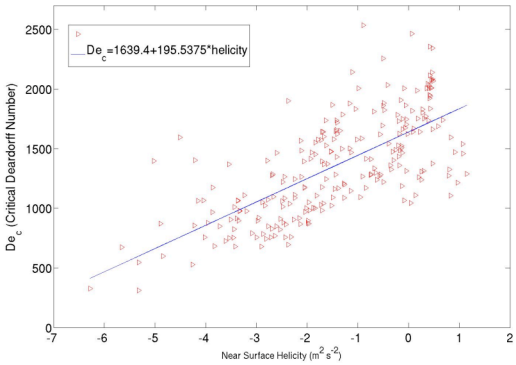


**Figure 5:** $De_c$ as a function of near-surface helicity at Amazonis Planitia ($F=239$, $p=1.1204*10^{-38}$)

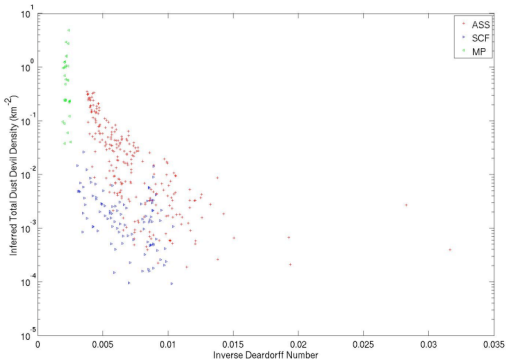


**Figure 6:** Arrhenius plot of $N_{DDT}$ vs. $De^{-1}$, combining data for all three sites (red: Amazonis Planitia; blue: Syria-Claritas Fossae; green: Meridiani Planum)

The relation still remains noisy but is suggestive. However, De and the inferred $De_c$ are closely related, but helicity more strongly anti-correlates with De than the inferred $De_c$, implying that the relation between $De_c$ and helicity may be coincidental.

**Consistency Between Sites:** One risk of any parameterization is that it will be overtuned to a particular data set. No parameterization scheme can be realistic if it works on one part of a planet but not elsewhere. Unfortunately, combining the datasets for all three sites suggests that we cannot develop a regionally consistent scheme with our present approach. In Figure 6, we present an Arrhenius plot of De for all the sites. Note that $N_{DDT}$ varies nearly three orders of magnitude at the same $De^{-1}$, which is a too large a difference to be explained by regional differences in wind shear climatology.

**Aerodynamic Roughness Length, A Key Uncertainty:** This analysis is subject to a large number of uncertainties, ranging from the possibility that the MRF convective boundary layer scheme used in MarsWRF is inappropriate for dry convection to concerns about dust storm activity creating differences between the model and real dust forcing. However, the most significant ones may be those associated with L. Provided Kurgansky [14] is correct about the size spectrum, much of the variability in MOC WA dust devil observations regionally may not represent variations in dust devil activity generally but may reflect regional differences in mechanical turbulence, which is a strong function of aerodynamic roughness length, i.e., $L \propto \ln(z_0^{-1})^3$. At present, we are investigating different techniques for inferring aerodynamic roughness length and the implications of different roughness forcings for Martian boundary layer temperatures and dust devil activity. This work is described in Heavens et al. [18] .

**References:** [1] S.K. Atreya et al. (2006), *Astrobiology*, **6**, 439-450. [2] S. Basu et al. (2004), *JGR*, **109,** E11006. [3] B.A. Cantor et al. (2006), *JGR*, **111**, E12002. [4] M.I. Richardson et al. (2006), AAS DPS meeting 38,70.04. [5] J.R. Murphy et al. (1995), *JGR*, **100** (E12), 26537-26376. [6] N.O. Renno et al. (1998), *J. Atmos. Sci.,* **55**(21), 3244-3252. [7] J.A. Fisher et al. (2005), *JGR*, **110,** E03004. [8] G.D. Hess and K.T. Spillane (1990), *J. Appl. Meteor.*, **29**, 498-507. [9] B.H. Fiedler and K.M. Kanak, *Atmos. Sci. Lett.*, doi:10.1006/asle.2001.0043. [10] R. Greeley and J.D. Iversen (1985), *Wind as a geological process*, Cambridge, UK: Cambridge UP. [11] S.R. Lewis et al. (1999), *JGR*, **104** (E10), 24177-24194. [12] T. Cortese and S. Balachandar (1993), *Phys. Fluids A*, **5**(12), 3226-3232. [13] V. Vesovic et al. (1990), *J. Phys. Chem. Ref. Data*, **19**(3), 763-808. [14] M.V. Kurgansky (2006), *GRL*, **33**, L19S06. [15] G.D. Hess et al. (1988), *J. Appl. Meteor.*, **27**, 305-317. [16] W.A. Lyons and S.R. Pease (1972), *Monthly Weather Review*, **100**(3), 235-237. [17] T. Maxworthy (1973), *J. Atmos. Sci.*, **30**, 1717-1722. [18] N.G. Heavens, M.I. Richardson, and A.D. Toigo (2007), *7th International Mars Conference*, submitted.

**Acknowledgments:** All MarsWRF simulations were performed on Caltech's CITerra cluster.